Food Research International 95 (2017) 9–18

Contents lists available at ScienceDirect

Food Research International

journal homepage: www.elsevier.com/locate/foodres

Thermal analysis methods for the rapid identification and authentication of swiftlet (*Aerodramus fuciphagus*) edible bird's nest – A mucin glycoprotein

Eric K.S. Shim, Gleen F. Chandra, Soo-Y. Lee *

Division of Chemistry & Biological Chemistry, School of Physical & Mathematical Sciences, Nanyang Technological University, 21 Nanyang Link, Singapore 637371, Singapore

ARTICLE INFO

Article history:
Received 16 January 2017
Received in revised form 8 February 2017
Accepted 26 February 2017
Available online 28 February 2017

Keywords:
Edible bird's nest
Thermogravimetric analysis
Differential scanning calorimetry
Adulterants

ABSTRACT

Edible bird's nest of the swiftlet *Aerodramus fuciphagus*, is an unusual dried mucin glycoprotein, which has been used, particularly by Asians, as a premium food and wide spectrum health supplement for centuries. For the first time, thermogravimetry, differential thermogravimetry, and differential scanning calorimetry methods are used for the rapid identification and authentication of edible bird's nest. It is shown that edible bird's nest has a total moisture content of 12.6% which is removed below 200 °C, followed by two major decomposition steps on heating under nitrogen gas. The first decomposition step (200–735 °C) has a mass loss of 68.0% with maximum rate of mass loss at about 294 °C, and the second decomposition step (735–1000 °C) has a mass loss of 15.4% with maximum rate of mass loss at about 842 °C, leaving a ceramic residue of about 4.0%. Differential scanning calorimetry shows that there are two kinds of bound water in edible bird's nest: (a) loosely bound water (about 7.5%) that dehydrates from edible bird's nest first, largely below 110 °C, which can also be removed by lyophilization, and (b) tightly bound water (about 5.0%), still present in the edible bird's nest after lyophilization, that dehydrates from edible bird's nest between 100 and 200 °C. The unique thermogravimetry and differential thermogravimetry curves of edible bird's nest serve as analytical standards and offer a simple, fast technique that requires only a small sample size (5–10 mg) without the need for sample pretreatment to authenticate and check for edible adulterants which may be introduced into edible bird's nest with a profit motive.

1. Introduction

The raw, white edible bird's nest (EBN) of the swiftlet of genus *Aerodramus* or *Collocalia fuciphaga* is built from a viscous, sticky secretion of mucin glycoprotein from a pair of sublingual glands beneath the tongue of the swiftlet. The strands of mucin glycoprotein are interlaced with feathers to form a strong composite material when dried to carry the weight of the eggs or hatchlings and a pair of parent swiftlets. The swiftlet is native to South East Asia, and the EBNs are built on the vertical walls of caves and, in more recent times, in man-made bird houses.

The raw EBN is soaked in water to facilitate removal of feathers, wood chips, egg shells, and tiny sand grains with tweezers, before being sold as cleaned, dried nest cement. Cleaned EBN is coveted and one of the most expensive foods in Chinese cuisine, and for that reason it has been termed "Caviar of the East" but it has no relation to fish eggs. It has been used as a health food in Chinese Medicine (CM) since the Tang dynasty (618–907 CE). EBN has about 10% by weight of sialic acid in the glycoprotein which could account for the many anecdotal health benefits associated with its consumption. One kg of the cleaned, dried EBN often retails for more than US$2000 today due to market forces of supply and demand. The high demand of EBN globally, especially from China, Hong Kong, and Taiwan has given rise to a large market valued at billions of US dollars annually.

EBN has been shown to be a mucin glycoprotein, a biopolymer, having the properties of both carbohydrate and protein by chemical tests (Wang, 1921). Structurally, the mucin glycoprotein is made up of a protein backbone with side chains of sugars, like a bottlebrush, as shown in Fig. 1 (Wieruszeski et al., 1987). By proximate analysis, it has been reported that ~62% by weight of EBN is protein built from 17 types of amino acids, ~28% is carbohydrates/sugars, and the rest are moisture (~8%), ash/minerals (~2%), and fat (<1%) (Marcone, 2005).

The high cost of EBN is a temptation for unethical suppliers to introduce cheaper edible adulterants into the EBN to boost profits. We have recently shown that the adulterants can be classified into two types (Shim, Chandra, Pedireddy, & Lee, 2016). Type I adulterants are solids which are rendered to have a similar appearance to EBN cement by the naked eye, and can be adhered externally to the surface of the nest cement. They may be largely polysaccharides or polypeptides, e.g. coralline seaweed, tremella fungus, and agar which are polysaccharides; and fish bladder and pork rind which are largely polypeptides. Such

* Corresponding author.
E-mail address: sooying@ntu.edu.sg (S.-Y. Lee).

http://dx.doi.org/10.1016/j.foodres.2017.02.018
0963-9969/

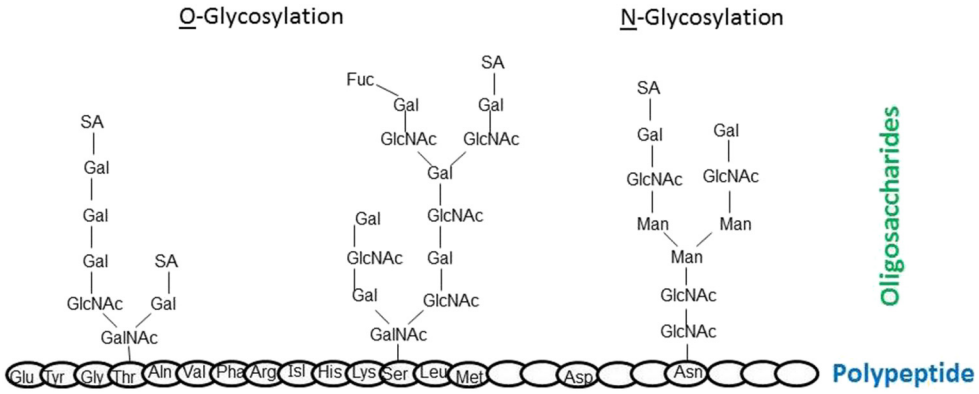

Fig. 1. Schematic representative of EBN mucin glycoprotein which contains both *N*- and *O*-glycosylproteins (Wieruszeski et al., 1987). A total of 17 types of amino acids: serine, valine, isoleucine, tyrosine, aspartic acid, asparagine, glutamic acid, glutamine, phenylalanine, arginine, glycine, threonine, alanine, lysine, histidine, leucine, and methionine make up the polypeptide backbone (Marcone, 2005). The major saccharides in the carbohydrate side chains are galactose (Gal), *N*-acetylneuraminic acid (Sialic Acid, SA), *N*-acetylgalactosamine (GalNAc), *N*-acetylglucosamine (GlcNAc), mannose (Man) and fucose (Fuc) (Ma & Liu, 2012).

adulterants tend to have a distinct difference in their microstructure from EBN and so that they can be detected with a microscope. On the other hand, Type II adulterants are water-soluble and can be absorbed by the EBN cement when it is soaked in the adulterant solution. They may be saccharides, polypeptides or salts, e.g. glucose and sucrose are saccharides, hydrolyzed marine collagen is a polypeptide, and monosodium glutamate is a salt. When the water is evaporated, the adulterants are incorporated into the EBN cement to form a new, uniform composite material. Such adulterated EBN has the same appearance as the unadulterated one under a microscope.

With the increasing occurrence of adulteration, there has been widespread interest in developing techniques to check for the quality and authenticity of EBN. Many physical, analytical and chemical techniques have been developed. For example, the microstructure of EBN fiber array was observed through microscopy and X-ray microanalysis (Marcone, 2005; Yang, Cheung, Li, & Cheung, 2014), and the shape of EBN was inspected by imaging analysis and machine vision technology (Ding, Zhang, & Kan, 2015). Separation techniques such as gas chromatography and liquid chromatography have been used to generate chromatographic metabolite mapping which reveal the composition of saccharides, amino acids and peptides to provide a chemical fingerprint for the EBN (Chua, Chan, Bloodworth, Li, & Leong, 2015; Hun et al., 2016; Saengkrajang, Matan, & Matan, 2013; Yang et al., 2014). Spectrophotometric methods (absorption and scattering spectroscopy) have been used to determine the sialic acid and protein content in EBN (Ma & Liu, 2012; Marcone, 2005). Enzymatic and genomic methods can detect some of the specific compounds present in EBN and differentiate heterogeneous protein from adulterants (Lin et al., 2009; Wu et al., 2010; Yang et al., 2014; Zhang et al., 2012), and the use of qualitative analysis to provide information on its constituents (Marcone, 2005). Through the use of these techniques, authentication of EBN may be achievable. However, many of the techniques require expensive instrumentation, large sample sizes and tedious sample preparation, and therefore may not be suitable for routine use.

EBN has not been studied before by thermal analysis. Thermogravimetry (TG) is a thermal analysis method in which changes in physical transition (to the gas phase) and chemical decomposition of a material is measured in terms of mass loss as a function of increasing temperature (with constant heating rate), as used here, or as a function of time in isothermal condition. TG and the corresponding differential thermogravimetry (DTG) have been useful for the study of complex materials like polymers and food substances (Huang et al., 2015; Manara et al., 2015; Santos et al., 2012; Siracusa, Blanco, Romani, Tylewicz, & Dalla Rosa, 2012; Torrecilla, García, García, & Rodríguez, 2011). Differential scanning calorimetry (DSC) technique is another appropriate thermal analysis method that measures the heat difference between sample and reference material to study thermo-physical transitions. It is has been used to study the thermal behavior of pharmaceutical and food systems to provide a predictive model for thermal stability with kinetic data (Blanco & Siracusa, 2013; Colombo, Ribotta, & León, 2010; Ruttarattanamongkol & Petrasch, 2016; Tolstorebrov, Eikevik, & Bantle, 2014; Vecchio, Cerretani, Bendini, & Chiavaro, 2009), and to detect adulteration in food products (Dahimi et al., 2014; Nur Azira & Amin, 2016; Tomaszewska-Gras, 2016). Both TG/DTG and DSC are useful tools for packaging materials and food characterization. They can provide rapid analysis with no sample pre-treatment and uses small quantities (5–10 mg). Here, we use thermal analysis by TG/DTG and DSC for the first time to study the thermal decomposition characteristics of EBN, the Type I adulterants, and new composite EBN incorporating Type II adulterants. The unique TG/DTG and DSC curves of EBN provide a reference to check for adulteration.

2. Materials and methods

2.1. Edible bird's nest (EBN) and adulterant samples

Raw, white EBN samples produced by the species *Aerodramus fuciphagus* were obtained from bird houses from different geographical locations in South-East Asia: Port Dickson (West Malaysia), Lahad Datu (East Malaysia), and Pekan Baru (Indonesia).

Coralline seaweed, tremella fungus, agar, fish bladder, and pork rind were purchased from grocery stores. Glucose, sucrose, hydrolyzed marine collagen and monosodium glutamate were purchased from suppliers of food chemicals and ingredients. Ultrapure water (18.2 MΩ cm) used in experiments was generated with the Merck Millipore ultrapure water system. The fish bladder and pork rind were cleaned of any remaining oil by soaking in warm water overnight, rinsed, and the moisture was squeezed out followed by air drying. Coralline seaweed and fish bladder were also bleached with 3% H_2O_2 solution for 30 min and air-dried to obtain a color to blend in better with EBN. All samples were kept at room temperature of 24 °C and relative humidity of 50%.

2.2. Microscope

Stemi 305 Trino Greenough system with Stand K EDU and spot illuminator K LED (Carl Zeiss) was used to obtain the microscopic images of EBN and Type I adulterants. The images were captured and recorded with Microscopy Camera Axiocam 105 color and ZEN Lite software (Carl Zeiss).

2.3. Thermogravimetric analysis (TGA)

Thermal Advantage Instruments TGAQ500 (TA Instruments) and the Universal Analysis software (TA Instruments) were used in acquisition and processing of the curves. Platinum sample crucible (100 μL, TA Instruments) was used as the sample container and the nitrogen gas flux was set at 60.0 mL/min to create a reproducible and dry atmosphere. About 3.0 to 4.0 mg of crushed powder from each sample was accurately weighed and placed on the tared platinum crucible. The crucible was then heated from 25 °C to 1000 °C and 800 °C for unadulterated and adulterated samples, respectively, at a heating rate of 15 °C/min.

The results were presented in curves of mass percentage versus temperature, TG curve, and the first derivative DTG curve which gave the rate of change of mass loss percentage (a positive number) versus temperature.

2.4. Differential scanning calorimetry (DSC)

Calorimetric measurements were performed with a DSCQ20 (TA Instruments) and the data processed with the same software used for TGA. The DSC profile was recorded as heat flow (W/g) versus temperature (°C). Calorimetric standards used for instrument calibration were indium and ultrapure water; 3.0–4.0 mg of powder form sample was sealed in a 40 μL aluminum Tzero pan and used for measurements. A purge flow (nitrogen gas) was maintained at 50 mL/min at all times. The standby temperature of the instrument was set at 40 °C, and each sample was then cooled from 40 °C to 0 °C and equilibrated for 60 s prior to measurement. The ramping rate (heating or cooling) was set at 5 °C/min. Triplicate analyses were carried out for each sample to ensure consistency in the results.

2.5. Uptake of Type II adulterants by EBN

Glucose, sucrose, hydrolyzed collagen, and MSG are water soluble and can be absorbed by the EBN cement. The adulterated EBN samples were prepared according to a recently reported procedure (Shim et al., 2016). About 1 g (weighed accurately) of EBN was soaked overnight in 50 mL of 1%, 2%, 5% or 10% solution of various Type II adulterants. Triplicate samples were made for each concentration of adulterant solutions. The samples were fan-dried at room temperature and 50% relative humidity for four days and then used for thermal analysis.

2.6. Principal component analysis (PCA)

Principal component analysis was performed by using the Origin 9.0 software (OriginLab). PC1 is using as the horizontal coordinate and PC2 as the vertical coordinate to generate a score plot.

3. Results and discussion

3.1. TG and DTG

Similar TG and DTG curves of EBNs from different geographical origins were obtained as shown in Fig. 2. Earlier, through the physical characterization of EBN by Raman microspectroscopy, it was shown that these EBNs also have a similar unique Raman spectrum indicative of a generally consistent biopolymer built of polysaccharides and polypeptides (Shim et al., 2016). The observation of unique TG and DTG curves for EBN is consistent with that finding.

There are three main regions in the curve. The first region from 25 to 200 °C corresponds to a physical dehydration of EBN. The DTG curve

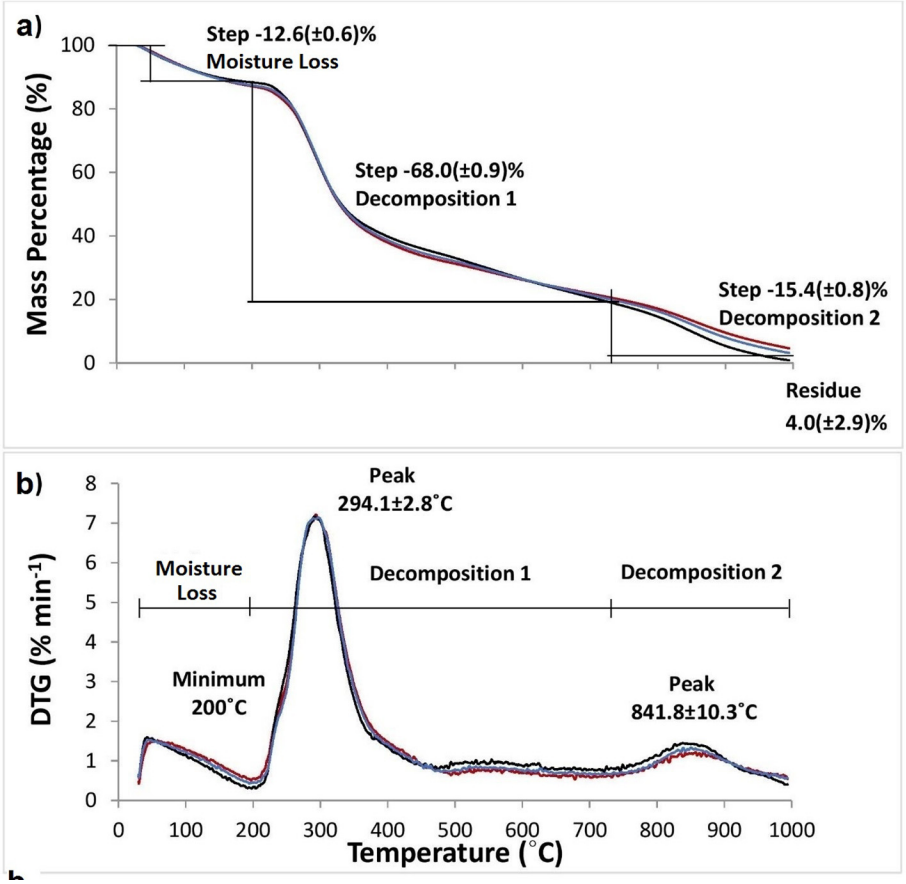

Fig. 2. a. Thermogravimetry (TG), and b. Differential thermogravimetry (DTG) curves of EBN samples collected from different geographical locations: (A). Port Dickson, West Malaysia (black line); (B). Lahad Datu, East Malaysia (red line); (C). Pekan Baru, Indonesia (blue line). (For interpretation of the references to color in this figure legend, the reader is referred to the web version of this article.)

presents a minimum at 200 °C and corresponds to a TG mass loss of 12.6(±0.6)% of moisture for raw EBN. By proximate analysis with drying to constant weight at 100 °C, Marcone reported that (white) EBN contained 7.5% moisture (Marcone, 2005). Indeed, on the TG curve, the loss of moisture is about 7.5% at 100 °C. As shown by the DSC study below, this loss of moisture corresponds largely to the loosely bound water, but EBN also has tightly bound water and it would require heating to 200 °C to remove both the loosely and tightly bound water.

After the complete loss of moisture at about 200 °C and on further heating, the DTG curve shows that there are two major regions where the anhydrous EBN chemically degrades with significant mass loss. The first chemical decomposition region is from 200 to 735 °C with a mass loss of 68.0(±0.9)%, and the DTG shows a maximum rate of mass loss at 294(±3) °C. The mass loss in this region is attributed to: (a) decarboxylation and bond breaking of the protein in the glycoprotein backbone which occurs at around 300 °C, as is also seen in collagen (Bozec & Odlyha, 2011; Tegza, Andreyeva, & Maistrenko, 2012), and (b) breakdown of the dendritic polysaccharide chains in the glycoprotein into smaller fragments, releasing volatiles and resulting in mass loss. In addition, the reducing sugar molecules in the polysaccharide chains of the glycoprotein can undergo the Maillard reaction with the amino acids from the protein chain in the presence of heat, and the volatiles released through the Maillard reaction also contribute to the mass loss.

The second decomposition region is from 735 to 1000 °C with a mass loss of 15.4(±0.8)%, and the maximum rate of mass loss is at 842(±10) °C. This high temperature region would correspond to the complex decomposition of multicomponent inorganic oxides, nitrates, and carbonates (Lehman, Gentry, & Glumac, 1998; Sayi et al., 2002; Stern, 1972; Tromp, Rubloff, Balk, LeGoues, & van Loenen, 1985). Swiftlets are insectivores scooping up airborne flying insects and ingesting sand and mineral rich water from a river for grinding their feed of insects in the gizzard, and these are primary sources of inorganic minerals in the EBN strands. Elemental analysis of EBN has shown the presence of calcium, sodium, magnesium, potassium, and iron ranging from tens to a thousand ppm (Marcone, 2005). Finally, at 1000 °C, a ceramic ash of 4.0(±2.9)% was obtained.

The unique TG and DTG curves of unadulterated EBN can be used to check for adulterants which may be introduced into EBN with a profit motive. In particular, there will be major differences in the DTG curves between unadulterated and adulterated EBNs.

3.2. DSC

The DSC curves, Figs. 3a–e, show that there are two kinds of bound water in EBN. Fig. 3a is the DSC curve for raw EBN heated from 0 to 400 °C. There is a broad endothermic band between 0 and 200 °C

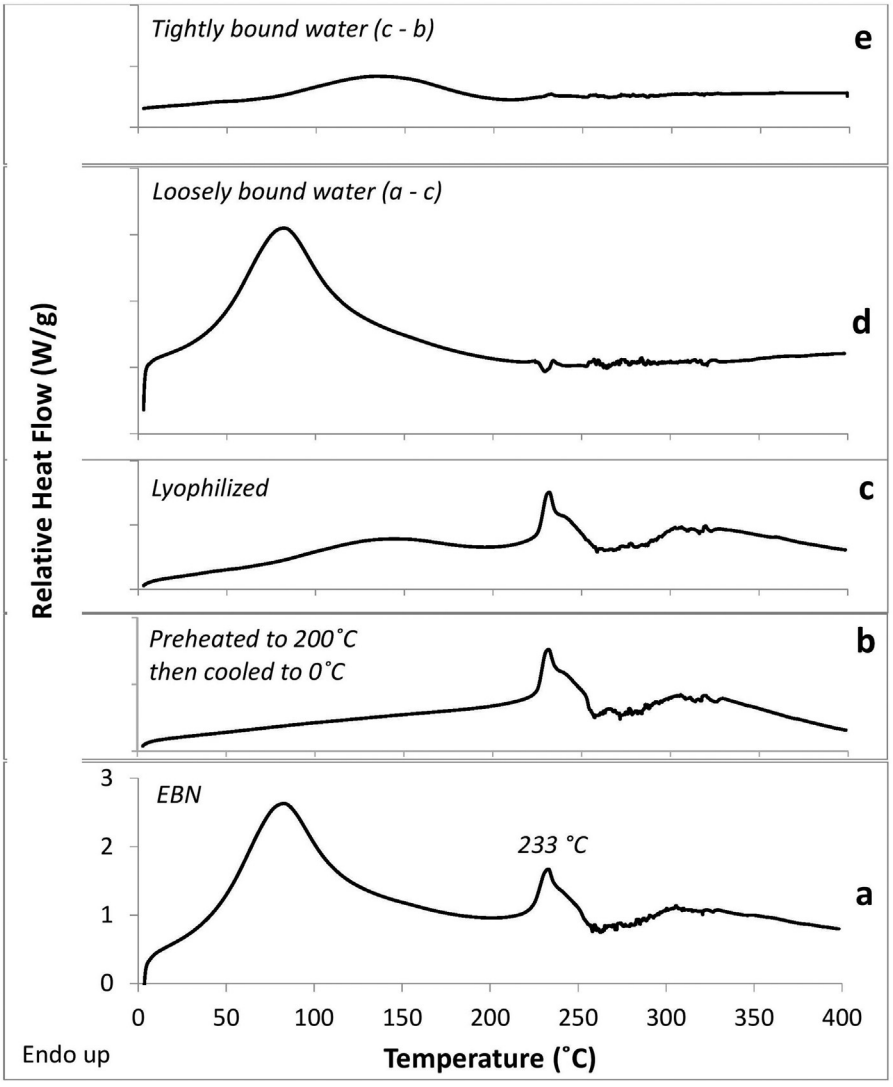

Fig. 3. DSC curves of Port Dickson EBN samples: a. raw EBN; b. EBN was first heated to 200 °C, then cooled to 0 °C; c. lyophilized EBN; d. the difference curve (a–c), showing the loosely bound moisture of EBN; e. the difference curve (c–b), showing the tightly bound moisture of EBN.

associated with the physical loss of water, with a peak at about 83 °C. This is followed by another endothermic band between 200 and 260 °C, with a relatively sharp peak at 233 °C which is due to the breakdown of the anhydrous EBN structure, akin to melting, with simultaneous chemical decomposition and volatilization. Subsequently, there's a broad endothermic band in the 260–400 °C range within the first decomposition stage of EBN as seen in the TG curve in Fig. 2.

Figs. 3b–e uses DSC to shed more light on the bound water. For Fig. 3b, the EBN was first heated to 200 °C to remove the bound water, cooled to 0 °C, and then DSC scanned from 0 to 400 °C. Clearly, water has been removed as seen from the straight line in the DSC curve (0–200 °C), and in the range of 200–400 °C is identical to that of Fig. 3a. For Fig. 3c, the EBN was first lyophilized to remove the loosely bound water, before the DSC scan from 0 to 400 °C. Here, we see that the lyophilization has removed the loosely bound water, leaving behind the more tightly bound water which appears in the range 83–200 °C, while from 200 to 400 °C it is identical to that of Fig. 3a and b. The TG curve of lyophilized EBN sample showed that it has about 5% by weight of tightly bound water, which means that the raw EBN has roughly 1.5:1 ratio of loosely bound to tightly bound water molecules.

By subtracting the DSC curve in Fig. 3c from Fig. 3a, we obtain the bell-shaped DSC curve for the loosely bound water shown in Fig. 3d, with an endothermic peak at 83 °C. Similarly, by subtracting the DSC curve in Fig. 3b from Fig. 3c, we obtain the bell-shaped DSC curve for the tightly bound water, shown in Fig. 3e, with a peak at 140 °C. The loosely bound water would correspond to water molecules surrounding the glycoprotein polymer and in between polymer chains, while the tightly bound water would correspond to the water molecules strongly hydrogen bonded with the polysaccharides and polypeptides in the coils of the glycoprotein chain.

This phenomenon of loosely bound and tightly bound water should be quite prevalent in food materials. Here, it has implications for the wide use of hydrogen peroxide, as a bactericide and bleaching agent in the bird nest cleaning industry. Some of the H_2O_2 may be tightly hydrogen bonded in the coils of the glycoprotein chains, just like the tightly bound water, and may remain trapped in the EBN on drying typically below 60 °C, and this could present a food hazard. It may be necessary to heat dry the cleaned EBN at above 100 °C to dislodge and decompose the hydrogen peroxide, or to reduce it in the moist EBN with permitted reducing agents like ascorbic acid, or by enzymatic decomposition with catalase, before drying.

3.3. Edible Type I adulterants in EBN

Edible Type I adulterants – coralline seaweed, tremella fungus, agar, fish bladder, pork rind – are solids which have some distinct differences in their surface structure that permit identification using a microscope. Coralline seaweed and fish bladder are naturally slightly pinkish red and yellow in color, respectively, but can be bleached with hydrogen peroxide (3% *w*/w) to obtain a translucent light yellow color to blend in with the EBN strands when added as adulterants. The microscopic images of EBN and the Type I adulterants are shown in Fig. 4. EBN has translucent strands of 0.5–1 mm diameter and each strand is made up of a few layers. Coralline seaweed has jointed branches of thickness about 1 mm and is opaque. Tremella fungus is whitish yellow, frond-like, and opaque. Agar strands are made of transparent, crumpled, thin sheets. Fish bladder and pork rind have an uneven, bubbly surface. EBN and the Type I adulterants soften when moist and the adulterants can be adhered to the EBN as strips or pieces using gelatin or hydrolyzed collagen as a glue.

The TG and DTG curves of these commonly used Type I adulterants are shown in Fig. 5. Clearly, the DTG band for each adulterant is unique and can be characterized by three parameters (temperature for the peak, peak height, and full width at half peak). Table 1 gives the unique set of parameters for the DTG bands of the adulterants in comparison with EBN. Coralline seaweed, tremella fungus, and agar are largely

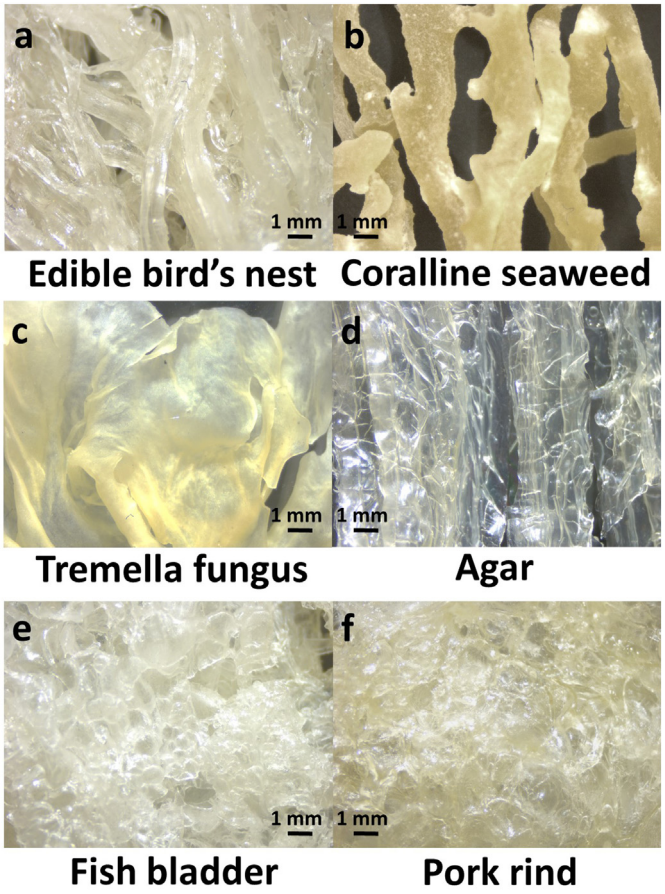

Fig. 4. Microscopic images of EBN and Type I adulterants: a. EBN; b. coralline seaweed; c. tremella fungus; d. agar; e. fish bladder; f. pork rind.

polysaccharides with the DTG maximum occurring at a lower temperature and overall a thinner band than that for fish bladder and pork rind which are largely polypeptides. It is also noted that agar shows two local maxima, with one of lower height than the other in the DTG curve. EBN being a glycoprotein has a temperature for the DTG maximum and a band width that falls between that of the polysaccharides and the polypeptides.

3.4. Composite of EBN with edible Type II adulterants

Type II adulterants are water soluble to give a transparent liquid which can be absorbed by the EBN, and on drying an amorphous composite material is obtained (Shim et al., 2016). The common Type II adulterants are glucose, sucrose, hydrolyzed collagen and monosodium glutamate (MSG). Glucose and sucrose are also used as sweeteners in the cooking of EBN; hydrolyzed collagen is added as a health supplement; and MSG is a taste enhancer. The presence of Type II adulterants cannot be detected with a microscope as they are embedded in the EBN matrix on drying without a change in physical appearance. However, TG and DTG in the temperature range of 25–500 °C can be used to detect the presence of Type II adulterants.

For each sample of unadulterated EBN, we know the moisture content based on its TG/DTG curves and so we can calculate the amount of anhydrous EBN cement. After soaking in the adulterant solution and fan drying, the new weight will comprise moisture, adulterant, and the same amount of anhydrous EBN cement. The amount of moisture is measured by TG/DTG, and we can thereby determine the amount of adulterant absorbed by the EBN cement. The average uptake of adulterants in the dried, composite EBN as a function of the concentration of adulterant solutions used are given in Table 2 and the results are plotted

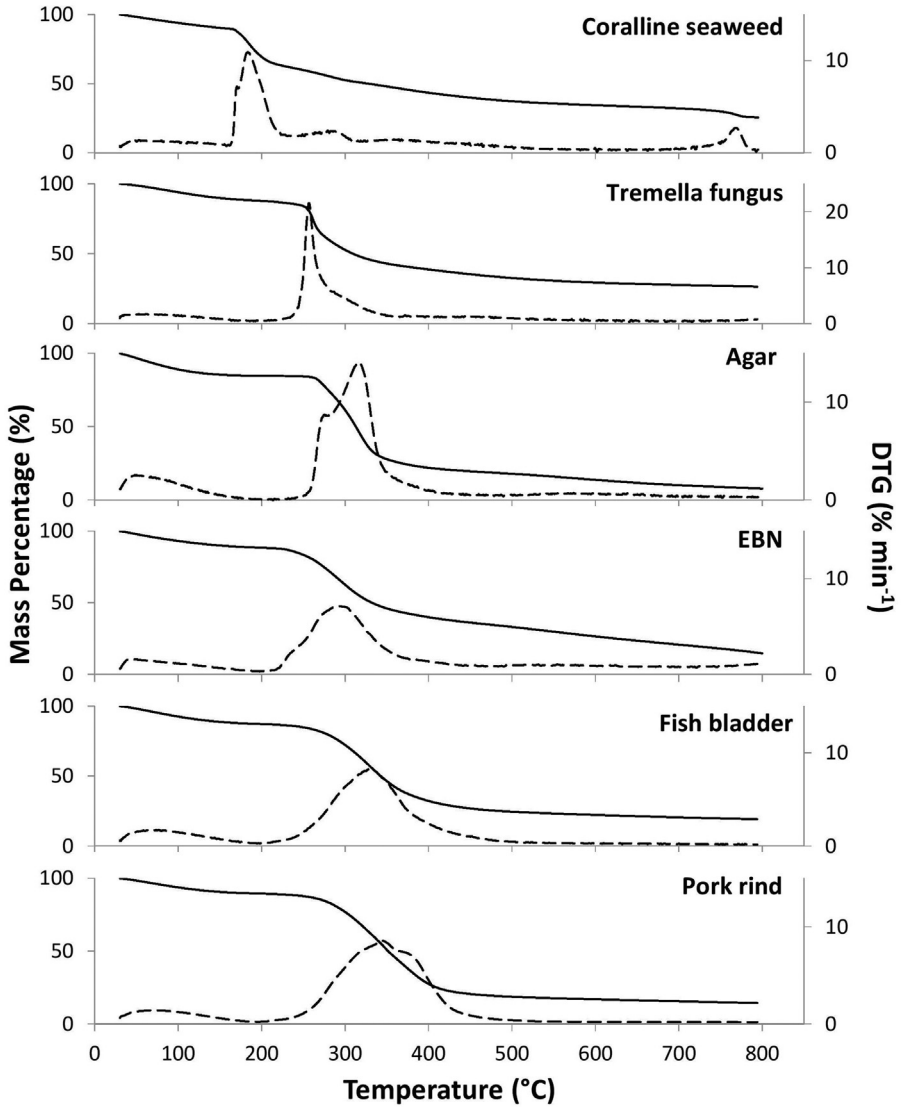

Fig. 5. TG (solid line) and DTG (dashed line) curves of various Type I adulterants – coralline seaweed, tremella fungus, agar, fish bladder, and pork rind – versus unadulterated EBN. The DTG peaks for the polysaccharides – coralline seaweed, tremella fungus, and agar – occur at a lower temperature than for EBN which is a glycoprotein, while those for the polypeptides – fish bladder and pork rind – occur at a higher temperature.

in Fig. 6. The uptake of the saccharides – sugar and glucose – can be quite substantial, with as much as 41% and 32% *w*/w of sugar and glucose embedded in the dried composite EBN when soaked in 10% *w*/w of adulterant solutions. Similarly, for hydrolyzed collagen as much as 30% *w*/w of collagen is absorbed in the composite with EBN, and for MSG about 22% *w*/w of MSG is absorbed. There's a good linear correlation between the amount of adulterant absorbed and the concentration of adulterant solution (up to 10% concentration) used to soak the EBN.

Table 1
Characterization parameters of DTG bands for Type I adulterants in comparison with unadulterated EBN.

Type I adulterant	Temperature of peak (°C)	Peak height (%/min)	Full-width at half peak (°C)
Coralline seaweed	182 ± 2	10.8 ± 0.1	33.7 ± 2.0
Tremella fungus	266 ± 1	22.4 ± 0.4	12.7 ± 0.9
Agar	275 ± 1, 316 ± 1	8.8 ± 0.2, 14.1 ± 0.1	64.0 ± 0.3
EBN	294 ± 3	7.2 ± 0.1	83.7 ± 1.6
Fish bladder	326 ± 3	8.5 ± 0.6	91.2 ± 4.0
Pork rind	344 ± 7	9.2 ± 0.2	105.5 ± 7.0

Table 2
Mass percentage of moisture and of Type II adulterants absorbed by EBN.

Type II adulterant	Concentration (*w*/w) of Type II adulterant solution	Mass percentage of moisture in composite EBN by TG (%)	Mass percentage of adulterant absorbed by EBN (%)
Glucose	1%	10.0 ± 0.2	4.5 ± 0.7
	2%	9.6 ± 0.2	8.1 ± 0.7
	5%	9.3 ± 0.7	17.8 ± 1.0
	10%	9.2 ± 0.3	33.9 ± 0.8
Sucrose	1%	9.9 ± 0.2	2.8 ± 0.7
	2%	9.0 ± 0.7	8.6 ± 1.0
	5%	7.8 ± 0.9	24.8 ± 1.2
	10%	6.1 ± 0.9	40.4 ± 1.2
Collagen	1%	10.1 ± 0.2	1.3 ± 0.7
	2%	10.3 ± 0.3	6.9 ± 0.8
	5%	10.7 ± 0.4	18.2 ± 0.8
	10%	11.1 ± 0.1	29.3 ± 0.7
Monosodium glutamate (MSG)	1%	10.2 ± 0.3	0.6 ± 0.7
	2%	10.0 ± 0.6	2.7 ± 0.9
	5%	10.6 ± 0.4	8.9 ± 0.8
	10%	10.0 ± 0.7	19.9 ± 1.0

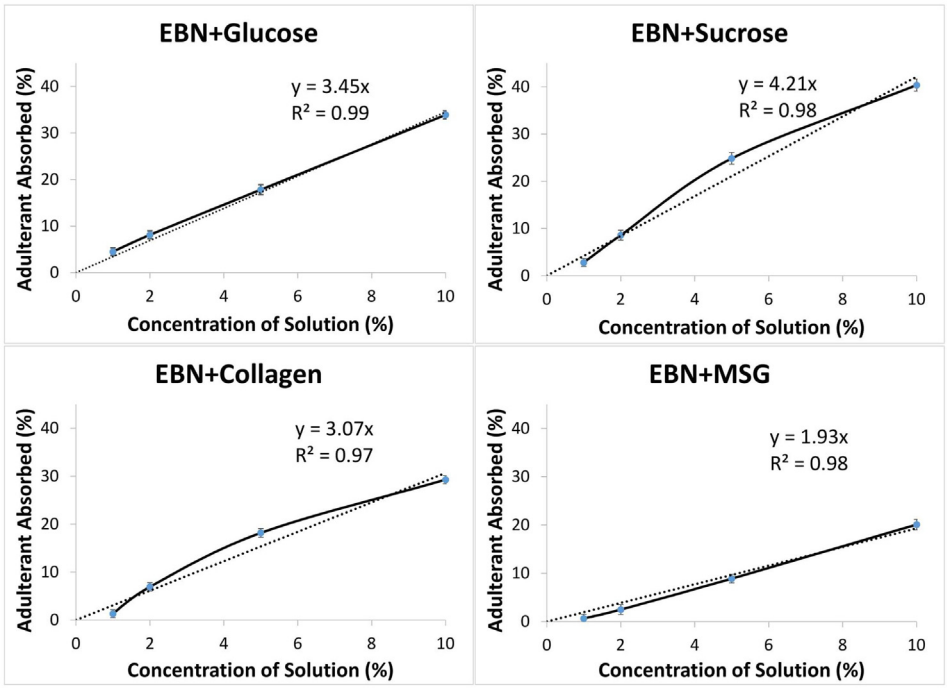

Fig. 6. Graphs of the uptake of Type II adulterants by EBN versus concentration of adulterant solutions used in soaking.

The TG and DTG curves for the dried, composite EBN previously soaked in different concentrations of adulterant solutions - 1%, 2%, 5% and 10% *w*/w - in comparison with unadulterated EBN are shown in Fig. 7. The DTG curves are presented as stack plots. The trends in the TG and DTG curves for increasing concentration of adulterant solutions are quite similar in the case of EBN + glucose and EBN + sucrose. Both involve simple sugars absorbed in the EBN matrix. Each set of the TG curves shows a significant difference in mass loss in the temperature range of 170–330 °C for increasing concentrations of adulterant solutions. The corresponding DTG curves show a peak around 190–220 °C due to the melting and decomposition of the sugars and Maillard reactions with the protein (which occur at a fast pace at temperature above 180 °C), and a corresponding decline in the band between 250 and 350 °C due to a decrease in the weight percentage of proteins (Benzing-Purdie, Ripmeester, & Ratcliffe, 1985; Chen, Liang, & Kitts, 2015).

Collagen is largely a protein, and since EBN has a high percentage of protein the TG curves for EBN + collagen and EBN are rather similar up to about 320 °C, but we note a general broadening of the DTG curves with increasing concentration of adulterant solutions. There is a slight increase in the new step at around 200–220 °C due to melting and decomposition. For the salt MSG, the TG curves for EBN + MSG do not fan out as pronounced as those for EBN + glucose and EBN + sucrose in the temperature range of 200–300 °C for the major decomposition step. The DTG curves show a new band at around 190–220 °C due to melting and decomposition. There are ripples on the DTG curves in the temperature range 300–350 °C, and the curves also broaden with increasing concentration of MSG solutions used. They can be attributed to the decomposition of dehydrated glutamate and pyroglutamate (Nunes & Cavalheiro, 2007).

The boxes in Fig. 7 show the regions in the DTG curves where the decomposition pattern of the adulterated EBN differ from the raw EBN. Generally, they fall under two main temperature ranges: (a) 175–220 °C, corresponding to melting and the onset of chemical decomposition, and (b) 250–350 °C, corresponding to the decomposition step with higher mass loss. The differences in the DTG curves between Type II adulterated and unadulterated EBN are summarized in Table 3. Clearly, the TG and DTG curves of the unadulterated EBN can be used as a reference to check for adulteration in EBN. From the TG and DTG curves, one can infer that the detection limit of adulteration by thermal analysis is at the 1% *w*/w of soaking solution where the adulterant is present at the 2–4% *w*/w concentration in the dry EBN.

Principal component analysis (PCA) is a statistical tool commonly used for data classification that is mathematically defined as an orthogonal linear transformation that transforms the data to a new coordinate system. As a result, the greatest variance lie on the horizontal coordinate (called the first principal component, PC1) and the second greatest variance is on the vertical coordinate (called the second principal component, PC2) in the score plot (Zhang, Qi, Zou, & Liu, 2011). In our study, a PCA of all the DTG curves for EBN samples soaked in 2%, 5% and 10% *w*/w aqueous solutions of Type II adulterants, and that of the unadulterated EBN from three different geographical regions, using the DTG data from 150 °C to 350 °C, was carried out.

The first four principal components are responsible for the major variations (>94%). PC1 and PC2 which accounted for variance of 65% and 15%, respectively, were used to plot the 2-D PCA scatter score plot shown in Fig. 8. By visual inspection, the separation among the data points can be observed along the PC1 horizontal axis and PC2 vertical axis. Samples with similarities are grouped together while dissimilar ones are spaced apart on the score plot. The formation of four clusters can be distinguished from Fig. 8. The first one is for EBN adulterated with collagen samples and unadulterated EBN as there are high similarities between DTG curves for marine collagen and EBN. The remaining three clusters are for EBN adulterated with glucose, sucrose, and MSG respectively, due to the characteristic DTG peaks for glucose (175–220 °C), sucrose (185–250 °C) and MSG (175–220 °C) arising from the decomposition of the adulterants. In agreement with the DTG curves in Fig. 7, EBN adulterated with 2% *w*/w aqueous solutions are at the borderline of thermal analysis sensitivity, and the PCA points tend towards that of the first cluster for EBN and EBN adulterated with collagen.

4. Conclusions

We have shown that the EBNs of the swiftlet *Aerodramus fuciphagus*, from widely different geographic regions, have unique thermogravimetric (TG) and differential thermogravimetric (DTG) curves. From

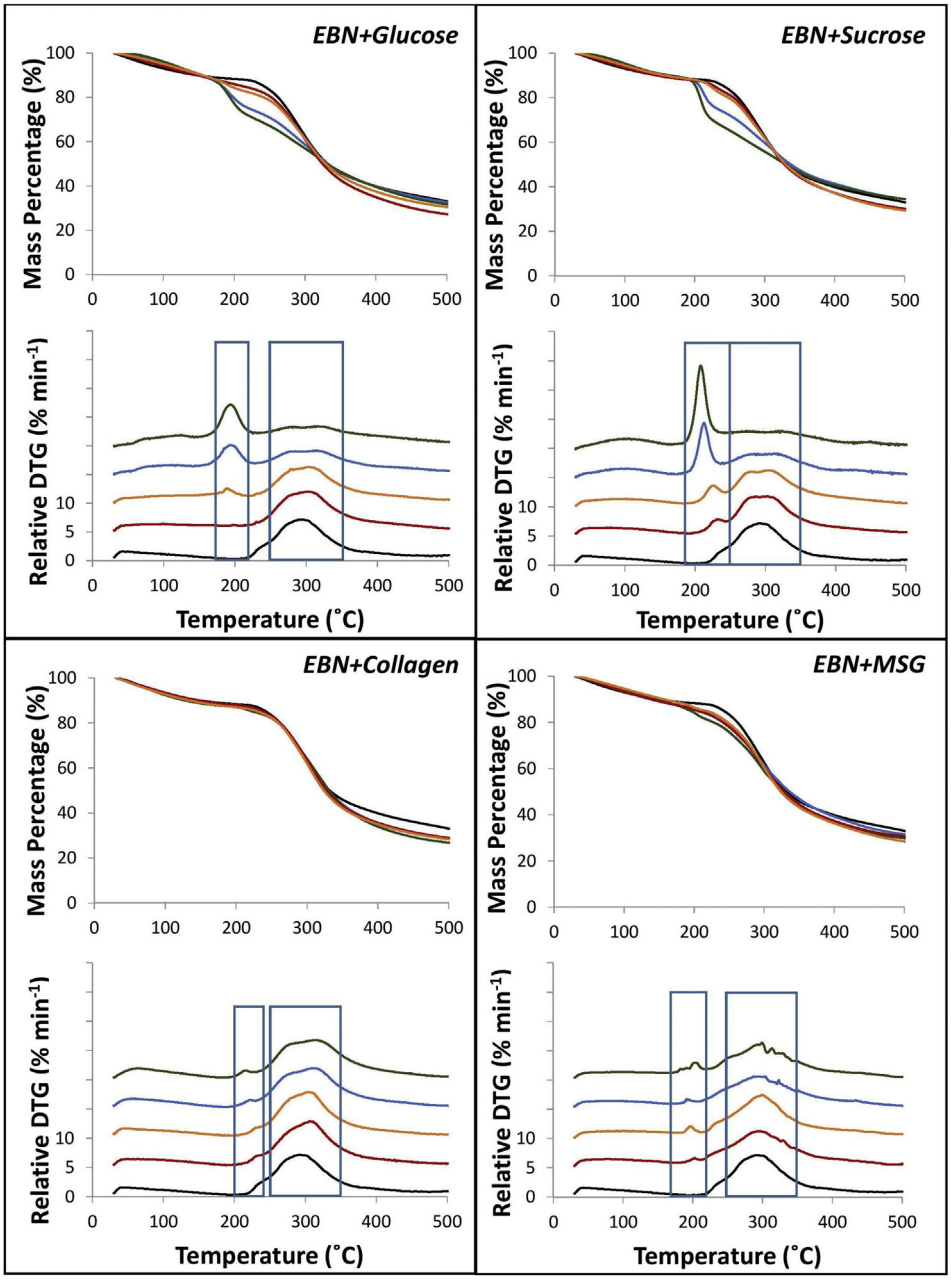

Fig. 7. TG and DTG curves of EBN adulterated with Type II adulterants. Each sub Fig. corresponds to a Type II adulterant: adulterated EBN prepared by soaking with 1% (red line), 2% (orange line); 5% (blue line) and 10% (green line) of Type II adulterant solutions. The comparison TG and DTG reference curves for unadulterated EBN are shown as black lines. The DTG curves are shown as stack plots, and the scale for the decomposition rate is for the unadulterated EBN. (For interpretation of the references to color in this figure legend, the reader is referred to the web version of this article.)

the TG and DTG curves, EBN is shown to have a total moisture content of 12.6%, which is about 5% higher than that reported in the literature by proximate analysis. Differential scanning calorimetry (DSC) showed that there are two kinds of bound water in EBN, and proximate analysis gives only the result for loosely bound water (7.5%). There is also about 5% of tightly bound water present in EBN. This finding should apply also to other food materials. The TG curve for EBN shows a main decomposition stage in the range of 200–735 °C with a peak at about 294 °C intermediate between that for polysaccharides and proteins which is consistent with EBN being a glycoprotein with both saccharides and proteins in the biopolymer.

Table 3
Comparison of DTG thermograms between Type II adulterated and unadulterated EBN.

Type II adulterant	Temperature range (°C) where the DTG curves are significantly different between adulterated and unadulterated EBN
Glucose	175–220 (new band); 250–350 (decreased band height)
Sucrose	185–250 (new band); 250–350 (decreased band height)
Collagen	200–240 (new band); 250–350 (broadened band)
Monosodium glutamate (MSG)	175–220 (new band); 250–350 (broadened band with ripples)

Thermal analysis provides a fast, easy to use technique requiring small sample sizes to detect adulteration in EBN. The adulterated EBN will have a different set of TG and DTG curves from that of the reference unadulterated EBN. Both Type I, surface adhered adulterants, e.g. coralline seaweed, tremella fungus, agar, fish bladder and pork rind which can be picked out with a microscope, and Type II water soluble adulterants, e.g. glucose, sucrose, hydrolyzed marine collagen, and MSG, which can be absorbed and bound inside the EBN matrix forming a uniform

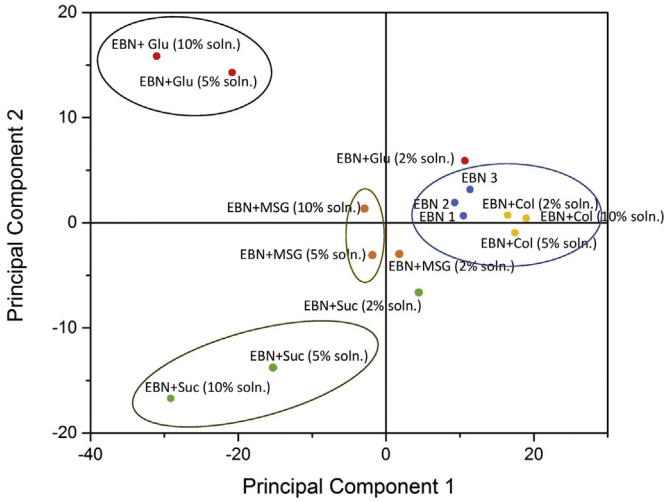

Fig. 8. Principal component analysis (PCA) score plot of the DTG data in the temperature range 150 °C to 350 °C, comprising: (A) the DTG of unadulterated EBN from three different geographical regions, (B) DTG of adulterated EBN, for samples soaked in 2%, 5% and 10% *w*/w aqueous solutions of glucose, sucrose, MSG and collagen. Four clusters appear in the PCA plot, consistent with the differences in the DTG curves for the various adulterants shown in Fig. 7.

composite material, can be detected by thermal analysis. The detection limit of Type II absorbed adulterants by thermal analysis is at the 2–4% *w*/w concentration, depending on the adulterant, in the dry EBN.

Conflicts of interest

The authors declare no conflicts of interest.

Acknowledgements

We gratefully acknowledge the financial support of the School of Physical and Mathematical Sciences, Nanyang Technological University, for consumables and instrument time.

References

Benzing-Purdie, L. M., Ripmeester, J. A., & Ratcliffe, C. I. (1985). Effects of temperature on Maillard reaction products. *Journal of Agricultural and Food Chemistry*, *33*(1), 31–33. http://dx.doi.org/10.1021/jf00061a009.

Blanco, I., & Siracusa, V. (2013). Kinetic study of the thermal and thermo-oxidative degradations of polylactide-modified films for food packaging. *Journal of Thermal Analysis and Calorimetry*, *112*(3), 1171–1177. http://dx.doi.org/10.1007/s10973-012-2535-8 (journal article).

Bozec, L., & Odlyha, M. (2011). Thermal denaturation studies of collagen by microthermal analysis and atomic force microscopy. *Biophysical Journal*, *101*(1), 228–236. http://dx.doi.org/10.1016/j.bpj.2011.04.033.

Chen, X. -M., Liang, N., & Kitts, D. D. (2015). Chemical properties and reactive oxygen and nitrogen species quenching activities of dry sugar–amino acid maillard reaction mixtures exposed to baking temperatures. *Food Research International*, *76*(Part 3), 618–625. http://dx.doi.org/10.1016/j.foodres.2015.06.033.

Chua, Y. G., Chan, S. H., Bloodworth, B. C., Li, S. F. Y., & Leong, L. P. (2015). Identification of edible bird's nest with amino acid and monosaccharide analysis. *Journal of Agricultural and Food Chemistry*, *63*(1), 279–289. http://dx.doi.org/10.1021/jf503157n.

Colombo, A., Ribotta, P. D., & León, A. E. (2010). Differential scanning calorimetry (DSC) studies on the thermal properties of peanut proteins. *Journal of Agricultural and Food Chemistry*, *58*(7), 4434–4439. http://dx.doi.org/10.1021/jf903426f.

Dahimi, O., Rahim, A. A., Abdulkarim, S. M., Hassan, M. S., Hashari, S. B. T. Z., Siti Mashitoh, A., & Saadi, S. (2014). Multivariate statistical analysis treatment of DSC thermal properties for animal fat adulteration. *Food Chemistry*, *158*, 132–138. http://dx.doi.org/10.1016/j.foodchem.2014.02.087.

Ding, Z., Zhang, R., & Kan, Z. (2015). Quality and safety inspection of food and agricultural products by LabVIEW IMAQ Vision. *Food Analytical Methods*, *8*(2), 290–301. http://dx.doi.org/10.1007/s12161-014-9989-1.

Huang, L., Chen, Y., Liu, G., Li, S., Liu, Y., & Gao, X. (2015). Non-isothermal pyrolysis characteristics of giant reed (*Arundo donax L.*) using thermogravimetric analysis. *Energy*, *87*, 31–40. http://dx.doi.org/10.1016/j.energy.2015.04.089.

Hun, L. T., Wani, W. A., Poh, H. Y., Baig, U., Ti Tjih, E. T., Nashiruddin, N. I., ... Aziz, R. A. (2016). Gel electrophoretic and liquid chromatographic methods for the identification and authentication of cave and house edible bird's nests from common adulterants. *Analytical Methods*, *8*(3), 526–536. http://dx.doi.org/10.1039/C5AY02170G.

Lehman, R. L., Gentry, J. S., & Glumac, N. G. (1998). Thermal stability of potassium carbonate near its melting point. *Thermochimica Acta*, *316*(1), 1–9. http://dx.doi.org/10.1016/S0040-6031(98)00289-5.

Lin, J. -R., Zhou, H., Lai, X. -P., Hou, Y., Xian, X. -M., Chen, J. -N., ... Dong, Y. (2009). Genetic identification of edible birds' nest based on mitochondrial DNA sequences. *Food Research International*, *42*(8), 1053–1061. http://dx.doi.org/10.1016/j.foodres.2009.04.014.

Ma, F., & Liu, D. (2012). Sketch of the edible bird's nest and its important bioactivities. *Food Research International*, *48*(2), 559–567. http://dx.doi.org/10.1016/j.foodres.2012.06.001.

Manara, P., Vamvuka, D., Sfakiotakis, S., Vanderghem, C., Richel, A., & Zabaniotou, A. (2015). Mediterranean agri-food processing wastes pyrolysis after pre-treatment and recovery of precursor materials: A TGA-based kinetic modeling study. *Food Research International*, *73*, 44–51. http://dx.doi.org/10.1016/j.foodres.2014.11.033.

Marcone, M. F. (2005). Characterization of the edible bird's nest the "Caviar of the East". *Food Research International*, *38*(10), 1125–1134. http://dx.doi.org/10.1016/j.foodres.2005.02.008.

Nunes, R. S., & Cavalheiro, É. T. G. (2007). Thermal behavior of glutamic acid and its sodium, lithium and ammonium salts. *Journal of Thermal Analysis and Calorimetry*, *87*(3), 627–630. http://dx.doi.org/10.1007/s10973-006-7788-7.

Nur Azira, T., & Amin, I. (2016). 12 - Advances in differential scanning calorimetry for food authenticity testing A2. In G. Downey (Ed.), *Advances in food authenticity testing* (pp. 311–335). Woodhead Publishing.

Ruttarattanamongkol, K., & Petrasch, A. (2016). Oxidative susceptibility and thermal properties of *Moringa Oliefera* seed oil obtained by pilot-scale subcritical and supercritical carbon dioxide extraction. *Journal of Food Process Engineering*, *39*(3), 226–236. http://dx.doi.org/10.1111/jfpe.12213.

Saengkrajang, W., Matan, N., & Matan, N. (2013). Nutritional composition of the farmed edible bird's nest (Collocalia fuciphaga) in Thailand. *Journal of Food Composition and Analysis*, *31*(1), 41–45. http://dx.doi.org/10.1016/j.jfca.2013.05.001.

Santos, O. V., Corrêa, N. C. F., Soares, F. A. S. M., Gioielli, L. A., Costa, C. E. F., & Lannes, S. C. S. (2012). Chemical evaluation and thermal behavior of Brazil nut oil obtained by different extraction processes. *Food Research International*, *47*(2), 253–258. http://dx.doi.org/10.1016/j.foodres.2011.06.038.

Sayi, Y. S., Yadav, C. S., Shankaran, P. S., Chhapru, G. C., Ramakumar, K. L., & Venugopal, V. (2002). Thermal decomposition of nitrogenous salts under vacuum. *International Journal of Mass Spectrometry*, *214*(3), 375–381. http://dx.doi.org/10.1016/S1387-3806(02)00542-0.

Shim, E. K. S., Chandra, G. F., Pedireddy, S., & Lee, S. -Y. (2016). Characterization of swiftlet edible bird nest, a mucin glycoprotein, and its adulterants by Raman microspectroscopy. *Journal of Food Science and Technology*, *53*(9), 3602–3608. http://dx.doi.org/10.1007/s13197-016-2344-3.

Siracusa, V., Blanco, I., Romani, S., Tylewicz, U., & Dalla Rosa, M. (2012). Gas permeability and thermal behavior of polypropylene films used for packaging minimally processed fresh-cut potatoes: A case study. *Journal of Food Science*, *77*(10), E264–E272. http://dx.doi.org/10.1111/j.1750-3841.2012.02905.x.

Stern, K. H. (1972). High temperature properties and decomposition of inorganic salts part 3, nitrates and nitrites. *Journal of Physical and Chemical Reference Data*, *1*(3), 747–772. http://dx.doi.org/10.1063/1.3253104.

Tegza, M., Andreyeva, O., & Maistrenko, L. (2012). Thermal analysis of collagen preparations. *Cheminė technologija*, *1*(59), 40–45.

Tolstorebrov, I., Eikevik, T. M., & Bantle, M. (2014). A DSC determination of phase transitions and liquid fraction in fish oils and mixtures of triacylglycerides. *Food Research International*, *58*, 132–140. http://dx.doi.org/10.1016/j.foodres.2014.01.064.

Tomaszewska-Gras, J. (2016). Rapid quantitative determination of butter adulteration with palm oil using the DSC technique. *Food Control*, *60*, 629–635. http://dx.doi.org/10.1016/j.foodcont.2015.09.001.

Torrecilla, J. S., García, J., García, S., & Rodríguez, F. (2011). Application of lag-k autocorrelation coefficient and the TGA signals approach to detecting and quantifying adulterations of extra virgin olive oil with inferior edible oils. *Analytica Chimica Acta*, *688*(2), 140–145. http://dx.doi.org/10.1016/j.aca.2011.01.009.

Tromp, R., Rubloff, G. W., Balk, P., LeGoues, F. K., & van Loenen, E. J. (1985). High-temperature SiO_2 decomposition at the SiO_2/Si interface. *Physical Review Letters*, *55*(21), 2332–2335.

Vecchio, S., Cerretani, L., Bendini, A., & Chiavaro, E. (2009). Thermal decomposition study of monovarietal extra virgin olive oil by simultaneous thermogravimetry/differential scanning calorimetry: Relation with chemical composition. *Journal of Agricultural and Food Chemistry*, *57*(11), 4793–4800. http://dx.doi.org/10.1021/jf900120v.

Wang, C. C. (1921). The composition of Chinese edible bird's nest and the nature of their proteins. *Journal of Biological Chemistry*, *49*(2), 429–439.

Wieruszeski, J. M., Michalski, J. C., Montreuil, J., Strecker, G., Peter-Katalinic, J., Egge, H., ... Vliegenthart, J. F. (1987). Structure of the monosialyl oligosaccharides derived from salivary gland mucin glycoproteins of the Chinese swiftlet (genus *Collocalia*). Characterization of novel types of extended core structure, Gal beta(1——3)[GlcNAc beta(1——6)] GalNAc alpha(1——3)GalNAc(-ol), and of chain termination, [Gal alpha(1——4)]0-1[Gal beta(1——4)]2GlcNAc beta(1——.). *Journal of Biological Chemistry*, *262*(14), 6650–6657.

Wu, Y., Chen, Y., Wang, B., Bai, L., Wu, R., Ge, Y., & Yuan, F. (2010). Application of SYBRgreen PCR and 2DGE methods to authenticate edible bird's nest food. *Food Research International*, *43*(8), 2020–2026. http://dx.doi.org/10.1016/j.foodres.2010.05.020.

Yang, M., Cheung, S. -H., Li, S. C., & Cheung, H. -Y. (2014). Establishment of a holistic and scientific protocol for the authentication and quality assurance of edible bird's nest. *Food Chemistry*, *151*, 271–278. http://dx.doi.org/10.1016/j.foodchem.2013.11.007.

Zhang, X., Qi, X., Zou, M., & Liu, F. (2011). Rapid authentication of olive oil by Raman spectroscopy using principal component analysis. *Analytical Letters*, *44*(12), 2209–2220. http://dx.doi.org/10.1080/00032719.2010.546030.

Zhang, S., Lai, X., Liu, X., Li, Y., Li, B., Huang, X., ... Yang, G. (2012). Competitive enzyme-linked immunoassay for Sialoglycoprotein of edible bird's nest in food and cosmetics. *Journal of Agricultural and Food Chemistry*, *60*(14), 3580–3585. http://dx.doi.org/10.1021/jf300865a.